Separation Science and Technology
Publication details, including instructions for authors and subscription information:
http://www.informaworld.com/smpp/title~content=t713708471

Modeling Batch Kinetics of Cadmium Removal: by a Recycled Iron Adsorbent

Edward H. Smith

To cite this Article Smith, Edward H.(1998) 'Modeling Batch Kinetics of Cadmium Removal: by a Recycled Iron Adsorbent', Separation Science and Technology, 33: 2, 149 — 168
To link to this Article: DOI: 10.1080/01496399808544761
URL: http://dx.doi.org/10.1080/01496399808544761

SEPARATION SCIENCE AND TECHNOLOGY, 33(2), pp. 149–168, 1998

Modeling Batch Kinetics of Cadmium Removal by a Recycled Iron Adsorbent

EDWARD H. SMITH
ENVIRONMENTAL ENGINEERING PROGRAM
MECHANICAL ENGINEERING DEPARTMENT
SOUTHERN METHODIST UNIVERSITY
DALLAS, TEXAS 75275-0337, USA
FAX: (214) 768-1473
E-MAIL: edhsmith@seas.smu.edu

ABSTRACT

The kinetics of cadmium adsorption onto a recycled iron-bearing material is investigated. Batch rate data are analyzed using a surface reaction rate model, solved analytically, and a dual rate diffusion model solved numerically. Experimental investigations examined the effects of sorbent particle size in the 0.06–0.5 mm diameter range and pH in the 4–7 range. While both rate models can describe time–concentration data for cadmium well, particularly for the larger granular sizes of sorbent, the analysis reveals a substantial variation in the relevant rate coefficients with particle radius, r, suggesting diffusion versus surface-controlled reaction kinetics. The second-order rate constant for the surface reaction model and the intraparticle diffusion coefficient of the dual rate diffusion model, represented as surface diffusion, were proportional to $1/r$.

Key Words. Adsorption; Batch kinetics; Cadmium; Diffusion; Iron fines; Surface reaction

INTRODUCTION

Metal oxides can be effective materials for removing metal contaminants in aqueous systems by sorption and/or filtration. For instance, natu-

ral zeolites have been utilized for removal of heavy metals in addition to iron and manganese (1–3). Potentially effective hybrid adsorbents are being developed using manganese or iron oxides as a primary or enhancing component (4, 5). Complex natural minerals such as vermiculite and glauconite have been shown to exhibit considerable capacity for adsorption of copper, zinc, cadmium, and lead (6, 7). More pure iron oxides are also effective in certain applications. Ferrihydrite is a common surface coating of subsoil particles and has been shown to have substantial adsorption capacity for cationic heavy metals and, under appropriate conditions, anionic species such as chromate and antimony (8–11). Processes for oxide coating of filter media and binding of iron hydroxides can provide treatment of heavy metals such as lead, cadmium, copper, chromium, and nickel from wastewater as well as soluble manganese from water supplies (12–14).

Waste shot blast fines, an iron-bearing material deriving from surface finishing operations in the manufacturing of cast-iron components, has recently been shown to demonstrate considerable potential for removal of heavy metals in aqueous waste streams (15). The material tests nonhazardous according to TCLP analysis, but is typically sent to a solid waste landfill for disposal, incurring associated transport and disposal costs in addition to consuming landfill space. Preliminary inspection of a sample of the material, however, reveals that it possesses a significant iron component with oxide surfaces that are effective sorption sites for metals in aqueous systems. Furthermore, isotherm studies for several heavy metals indicate that adsorption capacitites for shot blast fines exceed those reported for activated carbons and are comparable to values for metal oxides and some chelating polymeric exchangers (11, 16–18). The ready availability of the residual iron material renders its recycling and reuse as a sorbent a potentially innovative and cost-effective venture in certain pretreatment applications for metal-bearing wastewaters.

Laboratory-scale batch rate analyses can be used to evaluate kinetic and other parameters for the design of batch mode treatment systems given the desired treatment goals. The principal aims of this work are to: 1) experimentally investigate the adsorption rate of a divalent metal contaminant, cadmium, onto shot blast fines in batch systems; 2) to determine the effects of important system variables such as sorbent particle size and pH on adsorption rate; and 3) to examine the ability of two different rate models for describing the adsorption kinetics and thereby interpret and aid the understanding of experimental phenomena.

EXPERIMENTAL METHODS

Materials

A sample of waste shot blast fines was collected from an impact millroom wheelbrater at a cast-iron facility which produces ductile iron pipes and fittings. Composition of a composite sample of the material using microprobe analysis and confirmed by a total digestion analysis is 90–95% iron and iron oxides, ~1% manganese, up to 0.5% other metals, and the rest silica from casting residues. The Si versus Fe content may vary depending upon which unit in a plant is sampled, and this can affect the nature of the oxide layer subsequently formed in solution and its sorption properties (19, 20). Preparation of the recovered material for adsorption experiments involves sieving of various size fractions using US standard sieves and storing in air-tight glass containers. Material for immediate use is dried to a constant weight and stored in a desiccator. Otherwise, the fines were used in adsorption experiments as is. The size fractions collected ranged from 10/20 mesh size to 200/325. The 200/325 (0.044–0.075 mm diameter), 100/200 (0.075–0.15 mm diameter), 60/80 (0.18–0.25 mm diameter), and 30/40 (0.425–0.6 mm diameter) mesh sizes were utilized in the experiments reported in this study. Surface area was evaluated for the various size fractions by the three-point BET N_2 adsorption method using a Quantasorb surface analyzer. The surface area and other relevant properties of the solid prior to hydration have been given previously (21).

Synthetic wastewater was prepared from a concentrated stock solution of $Cd(NO_3)_2$ in deionized distilled water and an ionic background of 10^{-2} M as $NaClO_4$. All chemicals used were reagent grade. pH adjustment was with either 1 N $HClO_4$ or 1 N NaOH. The pH of working solutions for the kinetic studies was in the 4–7 range and was adjusted to the desired initial value after preparation in a 2-L volumetric flask. The samples were then sealed and set overnight. The following day the pH was readjusted to the desired initial value, if necessary, before proceeding with sorbent contact and the reaction period. By this procedure the initial pH of the solution is more firmly established in view of possible interactions with the ambient atmosphere. The pH was not adjusted during the reaction period, but any pH drift was measured and recorded. Cadmium analysis was by inductively coupled plasma (ICP) spectroscopy, employing four-point standard calibration prior to and following analysis of unknowns, and regular triplicate analyses to confirm the method. Analytical controls were maintained throughout including use of control and blank samples, mass balance checks, and minimization of losses incurred in transfer or solid separation steps. For instance, batch rate experiments were con-

ducted containing only shot blast fines in 10^{-2} M $NaClO_4$ solution with no cadmium at pH 4. Analysis of filtered samples for background cadmium associated with the fines yielded values less than the detection limit in every case.

Batch Rate Studies

Adsorption kinetics were evaluated in a continuously stirred, 2-L halar beaker with cover to limit any photocatalysis of the iron. All studies were conducted at 21 ± 2°C. Due to the intent of investigating the experimental sensitivity of the kinetics to specific variables, most notably particle size of the sorbent, an identical stirring rate of 500 rpm was used for all experiments. This was sufficient to keep the sorbent fines in suspension. There was a small but observable attrition of the iron-based fines over the course of an experiment as evidenced by the characteristic orange color imparted to the water. The majority of this was likely colloidal iron, as filtered samples had total soluble iron concentrations of between 0.05 and 0.5 ppm depending upon the experimental conditions.

Just prior to adding the iron fines to the stirred reactor, two unfiltered and two filtered aqueous samples were taken from the reactor to verify the initial target metal concentration and identify any filter losses of solute. A predetermined amount of iron sorbent was added to the test solution at time zero, and 5-mL samples were extracted from solution and filtered through a prewashed 0.45 μm membrane filter to separate the solid. The filtered solution was then adjusted to pH < 2 using 1 N $HClO_4$, and then analyzed for cadmium by ICP spectroscopy. By a mass balance assumption, the difference between the metal remaining and that initially present is considered adsorbed onto the solid. The pH of the solution was also monitored throughout since it is suspected that the presence of the solid, removal of metal from solution, and exposure to the atmosphere would result in some pH drift. Adsorption equilibrium information was required to model the adsorption kinetics. The experimental methods for acquiring this information have been detailed previously (15).

DATA EVALUATION AND DISCUSSION

Kinetic Models

Adsorption kinetics of aqueous phase metal removal onto oxide-bearing solids is normally assumed to be controlled by physical-chemical processes (i.e., diffusion) or by a more chemically dominant surface reaction. The latter may be represented by a second-order reaction of the form:

$$M + S \xrightarrow{k_s} MS \qquad (1)$$

where M represents the dissolved metal contaminant, S the available surface sites, MS the adsorbed state, and k the reaction rate constant (L^3/M-t). The rate equation is expressed in terms of the concentrations of respective reactants:

$$dC_M/dt = -k_s C_M C_S \tag{2}$$

Employing a Langmuir-type treatment (22), Eq. (2) can be rewritten entirely in terms of the liquid-phase metal concentration:

$$dC_t/dt = -k_s C_t(C_t - C^*) \tag{3}$$

In Eq. (3), C_M is no longer used since all concentrations refer to liquid-phase metal concentration in M/L^3 (note that the subscript t refers to time-variable quantities). The rate expression is now second order in C_t. $C_t - C^*$ represents an effective sorbent concentration remaining at time t, where C^* is the equilibrium concentration of solution-phase metal. C^* can be estimated from the equilibrium relationship and the sorbent dosage used in the experiment. Based on the solution to Eq. (3), the rate constant, k_s, may be determined by least-squares linear regression of $(1/C^*)\ln[(C_t - C^*)/C_t]$ versus t. The slope of this line is $-k_s$.

Diffusion-based kinetic models for adsorption typically derive from Fick's law (23). The liquid-phase mass balance for a completely mixed batch system incorporates the sorbent dosage.

$$V\frac{dC_t}{dt} = -W\frac{dQ_{ave,t}}{dt} \tag{4}$$

where V and W are the liquid volume and sorbent mass, respectively, and $Q_{avg,t}$ is the average concentration of metal in the sorbent phase at time, t. A dual mass transfer rate model considers both external, or liquid film, diffusion and intraparticle transport resistance. The solid-phase continuity equation assumes spherical sorbent particles and is of Fickian form.

$$\frac{\partial Q}{\partial t} = \frac{D_i}{r^2}\frac{\partial}{\partial r}\left(r^2\frac{\partial Q_{r,t}}{\partial r}\right) \tag{5}$$

where Q is the sorbent phase loading at r and t, r is the radial distance in the particle from its center, and D_i is an intraparticle diffusion coefficient that lumps all such processes into a single surface diffusion term. The initial conditions are that $C_{t=0} = C_0$ and $Q_{r,t=0} = 0$, where C_0 represents the initial concentration of metal prior to reaction. The boundary condition at the center of sorbent particles is that the solid-phase concentration gradient, $\partial Q_{r,t}/\partial t$, is zero. The condition at the particle surface equates the flux from the bulk phase to the liquid particle boundary layer, or film,

to the intraparticle flux, or:

$$k_f(C_t - C_{s,t}) = \rho D_i \frac{\partial Q_{r,t}}{\partial r} \quad (6)$$

where ρ is the particle density, k_f is the coefficient of film diffusion, and $C_{s,t}$ is the liquid-phase concentration at the sorbent surface in equilibrium with $Q_{R,t}$, and R is the particle radius. The external, k_f, and intraparticle, D_i, diffusion coefficients are determined by a best-fit calibration of the dynamic model with batch rate data. Models of this type have been used for simulating the dynamic removal of pollutants on other porous and slightly porous adsorbents, including granular iron oxide hybrids (12). Equations (4) and (5) can be solved efficiently by a numerical scheme using the initial and boundary conditions and the adsorption equilibrium relationship (15).

The equilibrium metal partitioning relationship is used to update $C_{s,t}$ at each time step in the simulation, and may be of a more classical form, $Q_e = f(C_e)$, where the subscript e denotes the equilibrium condition; or a more complex, fundamental approach such as surface complexation modeling may be used. For instance, Table 1 lists isotherm constants (K_F and n) for the simple Freundlich isotherm equation, $Q_e = K_F C_e^n$. The Freundlich expression has been used extensively to describe adsorption equilibria for heterogeneous surfaces and is relatively easy to incorporate into dynamic models. Trends in sorption capacity are largely captured in the parameter K_F, while n reflects the steepness in a plot of equilibrium solid- versus liquid-phase concentration whether presented in an arithmetic or logarithmic format. The values in Table 1 indicate that cadmium isotherm capacity varies little for the 200/325, 100/200, and 60/80 mesh

TABLE 1
Freundlich Isotherm Coefficients for Cd Adsorption onto Shot Blast Fines
(all solutions C_0 = 5 mg/L Cd and 0.01 M $NaClO_4$)

Mesh size	d_{avg}[a] (mm)	pH	K_F[b]	n[b]
200/325	0.06	7.0	7.96	0.105
200/325	0.06	5.5	6.91	0.071
200/325	0.06	4.0	4.66	0.202
100/200	0.11	7.0	8.14	0.112
60/80	0.21	7.0	8.04	0.269
30/40	0.51	7.0	19.7	0.143

[a] Average diameter of fines.
[b] Based on $Q_e = K_F C_e^n$, where C_e is in mg/L and Q_e is in mg/g.

size particles. The 30/40 fraction, however, exhibits a markedly higher capacity as given by a K_F value of 19.7 versus ~8.0 for the other three sizes. The reason(s) for this difference are not clear at this time; composition studies of respective fractions are being undertaken to gain insights into this result. Table 1 also presents isotherm constants for cadmium adsorption at several initial pH values for the powdered sized (200/325 mesh) sorbent particles, since these are referred to in the following section on the effects of pH on adsorption rate. As expected, cadmium adsorption capacity increases with pH in the 4–7 range, reflected in increasing K_F with pH.

pH variations in adsorption equilibria can be described in a more fundamental sense by a surface complexation mechanism. It is observed that when placed in solution, a hydrous oxide layer forms over time on the surface of the shot blast fines, albeit in a heterogeneous fashion as illustrated in Fig. 1 for 60/80 mesh particles 2 hours after contact with solution. As a result, the material is assumed to have oxide or hydroxylated surface sites in solution, in particular $>FeOH_2^+$, $>FeOH$, and FeO^- representing positively charged, neutral, and negatively charged sites, respectively. The aqueous phase distribution of these surface species is given by the following protolysis equilibria.

$$>FeOH_2^+ \rightleftharpoons >FeOH + H^+, \quad K_{s1} = \frac{[>FeOH][H^+]}{[>FeOH_2^+]} \exp(-F\Psi_o/\hat{R}T) \tag{7}$$

$$>FeOH \rightleftharpoons >FeO^- + H^+, \quad K_{s2} = \frac{[>FeO^-][H^+]}{[>FeOH]} \exp(-F\Psi_o/\hat{R}T) \tag{8}$$

The surface protolysis constants, K_{s1} and K_{s2}, as given here include an electrostatic contribution. In the electrostatic term, F is the Faraday constant, $\hat{R}$ is the universal gas constant, T is absolute temperature, and Ψ_o is the average potential of the near-surface (or o-plane) as postulated by the Stern–Grahame modification of the Gouy–Chapman description of the electrical double layer (24). K_{s1} and K_{s2} can be estimated by calibration of a mathematical model of the system of solution-phase equations that includes (7) and (8) with potentiometric titration data for the sorbent in background electrolyte only. Based on observations of variations with the concentration of background electrolyte, in this case $NaClO_4$, a triple-layer model of the sorbent particle surface was used since it is designed to capture these effects. Therefore, surface interactions with Na^+ and ClO_4^- are also included in the species distribution calculations. If inner layer surface complexes are used to simulate cadmium adsorption equilib-

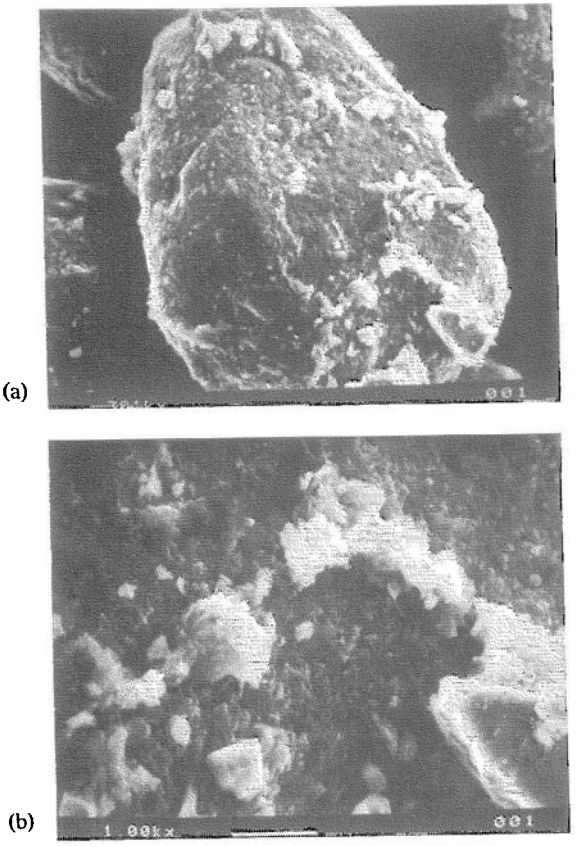

FIG. 1 Heterogeneous hydrous oxidation pattern of a 60/80 mesh particle at magnifications (a) 300 and (b) 1000, using an ISI-SX-25 SEM.

ria as a function of pH, a proposed mechanism of surface complexation of Cd^{2+}, the predominant soluble species at pH < 7, is

$$>FeOH + Cd^{2+} \rightleftharpoons >FeOCd^{+} + H^{+}$$

$$K_{ads} = \frac{[>FeOCd^{+}][H^{+}]}{[>FeOH][Cd^{2+}]} \exp(F\Psi_o/\hat{R}T) \tag{9}$$

The equilibrium constant, K_{ads}, represents the partitioning coefficient for cadmium between the solution and sorbent phases for a given sorbent dosage and is obtained by calibration of a model comprised of the above

equations with pH–adsorption data; i.e., adsorption edges. An example of values for the protolysis, electrolyte surface, and adsorption reactions is given in Table 2 for cadmium adsorption onto 200/325 mesh fines. Details of the experiments, experimental data, and computational procedures are presented elsewhere (15, 21).

Although more difficult, a surface complexation description of adsorption equilibria can be integrated into time-advancing rate models such as those employed in this study. A recent effort by the author has demonstrated that the use of either the surface complexation approach or a more simple equilibrium expression, such as the Freundlich or Langmuir, will produce essentially identical batch rate model simulations provided that pH dynamics are properly incorporated (15). In other words, if batch rate data are to be simulated according to the equilibrium (versus initial) pH of the system, then the isotherm constants used in kinetic modeling must correspond to that equilibrium (versus initial) pH value.

Evaluation

Batch rate data and model simulations are presented in Fig. 2(a) for 200/325 mesh shot blast fines (diam.$_{avg}$ = 0.06 mm) for a 5-mg/L Cd solution in 0.01 M $NaClO_4$. The data reveal a rapid adsorption rate of Cd, with virtual equilibrium attained within approximately 5–8 hours. This initial metal uptake, however, is slower than the 5–30 minute initial uptake step re-

TABLE 2
Equilibrium Constants for Triple Layer Modeling of Cd pH–Adsorption Edges

	Log K
Surface acidity reactions:	
$\equiv FeOH + H^+ \rightleftharpoons \equiv FeOH_2^+$	6.35
$\equiv FeOH \rightleftharpoons \equiv FeO^- + H^+$	−10.65
Electrolyte surface reactions:	
$\equiv FeOH + H^+ + ClO_4^- \rightleftharpoons (\equiv FeOH_2^+ - ClO_4^-)$	9.00
$\equiv FeOH + Na^+ \rightleftharpoons (\equiv FeO^- - Na^+) + H^+$	−9.78
Inner layer surface reactions:	
$\equiv FeOH + Cd^{2+} \rightleftharpoons \equiv FeOCd^+ + H^+$	1.50
Hydrolysis reactions:[a]	
$Cd^{2+} + H_2O \rightleftharpoons CdOH^+ + H^+$	−10.03
$Cd^{2+} + 2H_2O \rightleftharpoons Cd(OH)_2 + 2H^+$	−20.35
$Cd^{2+} + 3H_2O \rightleftharpoons Cd(OH)_3^- + 3H^+$	−33.30

[a] Reference: C. F. Baes and R. E. Mesmer, *The Hydrolysis of Cations*, Wiley, New York, NY, 1976.

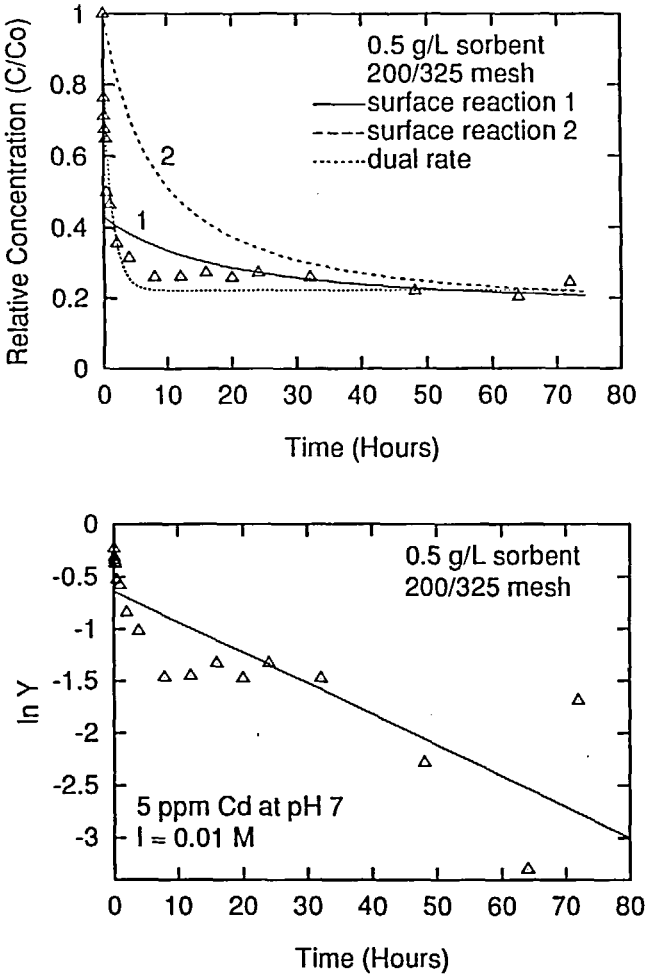

FIG. 2 (a) Batch rate data and surface reaction vs dual rate model simulations for C_0 = 5 ppm Cd(II), initial pH 7, 0.01 M ionic strength. (b) Semilog plot for determination of k_s according to Eq. (13).

ported for more pure iron oxides (11). Two different surface reaction model curves appearing in Fig. 2(a) are based upon implementation of the solution to Eq. (3) which is the following:

$$\frac{1}{C^*}\ln\left(\frac{C_t - C^*}{C_t}\right) = -kt + \frac{1}{C^*}\ln\left(\frac{C_0 - C^*}{C_0}\right) \qquad (10)$$

The second term on the right-hand side of Eq. (10) is a constant term and a function of the effective total sorbent concentration available at the start of the run, $C_0 - C^*$. If this term is not considered and the linear regression exercise is permitted to independently compute an intercept from $(1/C^*)$ $\ln[(C_t - C^*)/C_t]$ versus t, the result is the curve labeled 1 in Fig. 2(a). The linearization for estimation of k_s is illustrated in Fig. 2(b), where Y is the left-hand side of Eq. (10). Although this analysis provides a suitable description of data for advancing time, it does not capture the steep concentration gradient of the early removal stage. The discrepancy between the calculated intercept and that given directly by Eq. (10) is indicative of the inability of the surface reaction model to describe the adsorption kinetics of cadmium onto small diameter fines. This is also depicted by the nonlinear pattern/scatter of the points in the semilog plot of Fig. 2(b).

The surface reaction model curve 2 in Fig. 2(a) includes the right-hand side term of Eq. (10) in the calculation of k_s. This yields the same value of k_s as the previous analysis, but forces the model solution through the true starting position, namely $C/C_0 = 1$ at time zero. While this approach yields a more realistic picture of the entire kinetic profile, it does not capture the rapid rate of adsorption during the early minutes of the experiment. By contrast, the dual rate diffusion-based dynamic model is capable of tracing both the rapid initial removal and immediate leveling of the time–concentration data as the run proceeds. Like many instances of

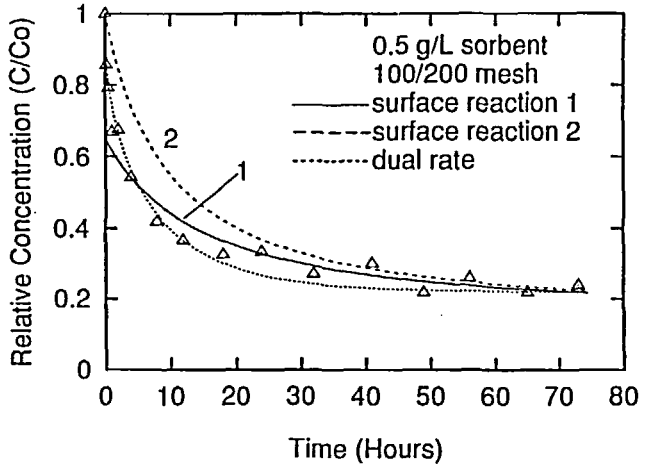

FIG. 3 Batch rate data and surface reaction vs dual rate model simulations for $C_0 = 5$ ppm Cd(II), initial pH 7, 0.01 M ionic strength.

metal adsorption onto powdered-sized porous sorbents, the results suggest that the rate of actual surface attachment is fast and not reaction limited. A more certain analysis, however, requires examination of uptake rates as a function of sorbent particle size.

Figure 3 shows rate data and comparative model simulations for 100/200 mesh sorbent (diam.$_{avg}$ = 0.11 mm). Once again there is a rapid initial removal of Cd, although this region is not as sharply delineated as in the case of the smaller fines, and extends over a longer (10–20 hours) period. Another contrast is that a slow uptake of metal continues beyond the initial period for another 30–50 hours before attainment to an apparent equilibrium condition. As indicated in Fig. 3, the surface reaction model provides a better description of time–concentration data than in the previous case, although the simulations representing the two methods used to develop the surface model curve still deviate substantially. The dual rate model simulation is also shown and, as before, provides a better fit of the data over the entire profile. Rate coefficients for the two modeling schemes are presented in Table 3 (note that the cases described above are for an initial solution pH of 7). The surface rate constant k_s is ~25% less for the 0.11 versus 0.06 mm diameter fines. The intraparticle diffusion coefficient D_i, however, is less than half the value of the smaller particle size. The variation of the rate constants with sorbent particle size is indicative of diffusion-controlled adsorption kinetics.

TABLE 3
Rate Coefficients for Surface Reaction and Diffusion-Based Rate Models
(all solutions C_0 = 5 mg/L Cd and 0.01 M $NaClO_4$)

Mesh size	d_{avg}[a] (mm)	pH	Dose (g/L)	Surface model, $k_s \times 10^3$ (L/mg·h)	Diffusion model, $k_f \times 10^3$ (cm/s)	Diffusion model, $D_i \times 10^{11}$ (cm^2/s)
200/325	0.06	7.0	0.5	29.6	4.5	15.0
200/325	0.06	5.5	0.5	32.2	5.0	7.5
200/325	0.06	4.0	0.5	27.9	4.5	4.5
100/200	0.11	7.0	0.5	22.4	4.6	6.9
60/80	0.21	7.0	0.5	10.6	4.0	3.5
30/40	0.51	7.0	0.4	3.43	4.0	2.4

[a] Average diameter of fines.

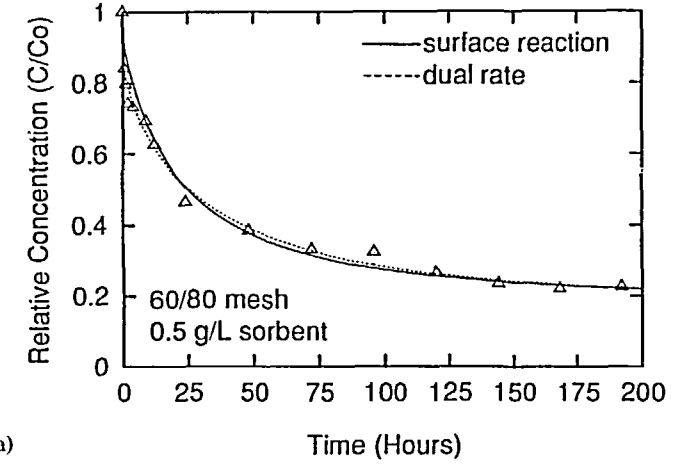

(a)

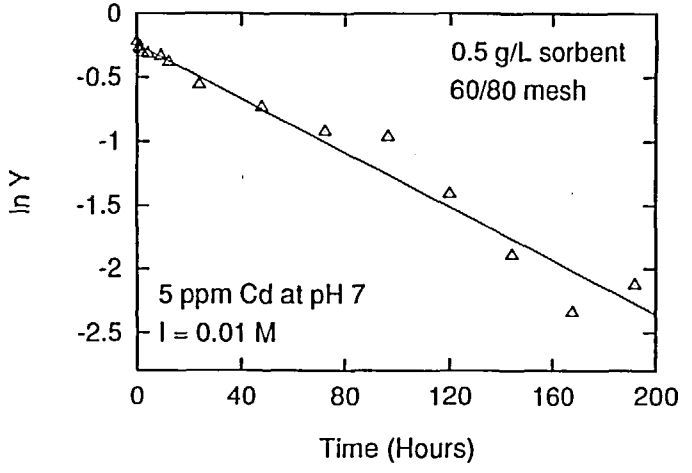

(b)

FIG. 4 (a) Batch rate data and surface reaction vs dual rate model simulations for C_0 = 5 ppm Cd(II), initial pH 7, 0.01 M ionic strength. (b) Semilog plot for determination of k_s according to Eq. (13).

This hypothesis was further tested by experiments with two larger grain sizes. Figures 4(a) and 5 contain rate data and surface versus dual rate kinetic model simulations for 60/80 mesh ($diam._{avg}$ = 0.21 mm) and 30/40 mesh ($diam._{avg}$ = 0.51 mm) sorbent fines, respectively. There is essentially no difference in the ability of the models to accurately simulate the adsorption rate data for Cd for either case. In fact, the two methods described previously for developing the surface model curve essentially converge. Figure 4(b) also illustrates the diminished scatter in the semilog fit used to estimate k_s. This implies a higher certainty in the parameter estimate as reflected in the more narrow 95% confidence bands for k_s of 9.4–11.7 $\times$ 10^{-3} for 60/80 mesh particles versus 19.7–39.4 $\times$ 10^{-3} for 200/325 fines. Consistent with Figs. 2(a) and 3, there is an increasingly slower approach to equilibrium as the size of sorbent particles increases. In Table 3, k_s and D_i also show a patterned decrease for increasing grain size of the sorbent, lending stronger confirmation to a diffusion-controlled reaction rate. The approximate inverse proportionality of k_s and D_i to the particle radius, r, is illustrated in Figs. 6(a) and (b). The film diffusion coefficient, k_f, is not appreciably affected by particle size of the sorbent.

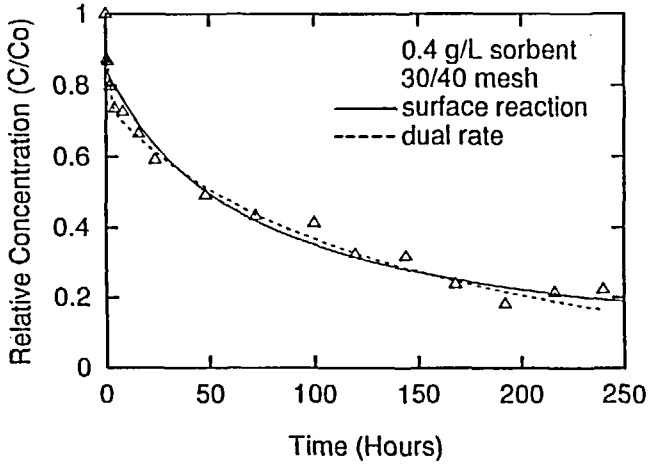

FIG. 5 Batch rate data and surface reaction vs dual rate model simulations for C_0 = 5 ppm Cd(II), initial pH 7, 0.01 M ionic strength.

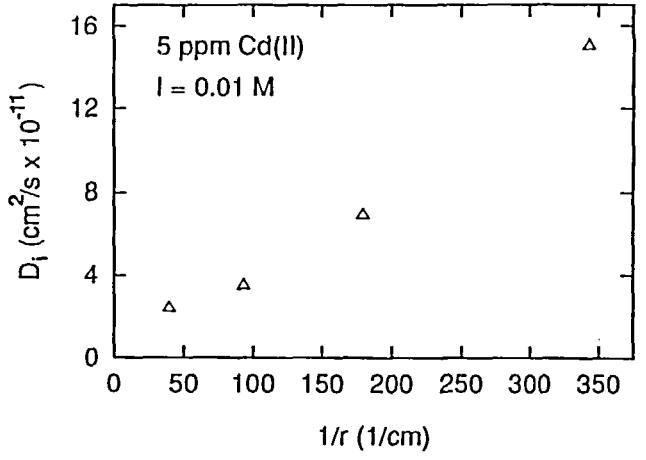

(a)

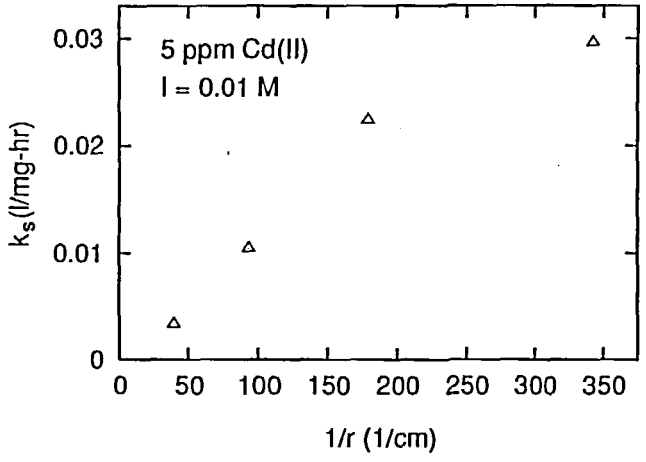

(b)

FIG. 6 Relationship of (a) surface reaction coefficient, k_s; and (b) intraparticle diffusion coefficient, D_s, to $1/r$.

Since pH is highly determinative of metal adsorption, the pH was monitored throughout all batch rate experiments. Figure 7 shows pH variations for several batch rate studies using different sorbent particle sizes. The pH dropped quickly from an initial value of 7.0 to about 6.4 for 200/325 mesh fines and to 6.5–6.6 for the larger sizes, where it remained essentially steady for the remainder of the sampling period. The results in Table 3 indicate that variations in pH have little impact on k_s for the powdered (200/325 mesh) fraction. Dual rate intraparticle mass transfer, however, appears to decrease with decreasing pH. The change of D_i with pH is likely due in part to the relationship of pH to the evolution of the oxide layer on the solid, thereby also impacting the nature of mass transfer in and among the oxide layer/particle core interface. In addition, due to the fairly rapid attainment of equilibrium for the powdered fraction, the model curve is only moderately sensitive to changes in D_i compared to a high sensitivity for larger sorbent particles. This is illustrated in the sensitivity analyses of Figs. 8(a) and (b) for the 0.5 g/L dosage case using 200/325 and 60/80 mesh sizes, respectively. Further study is required to more fully understand these relationships.

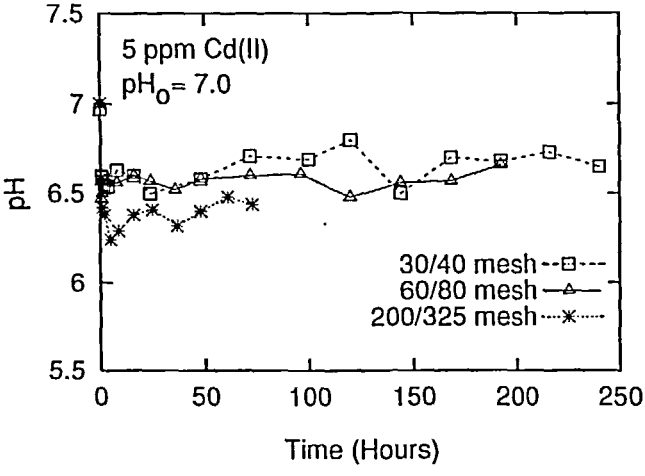

FIG. 7 pH drift in batch rate studies for different sorbent particle sizes.

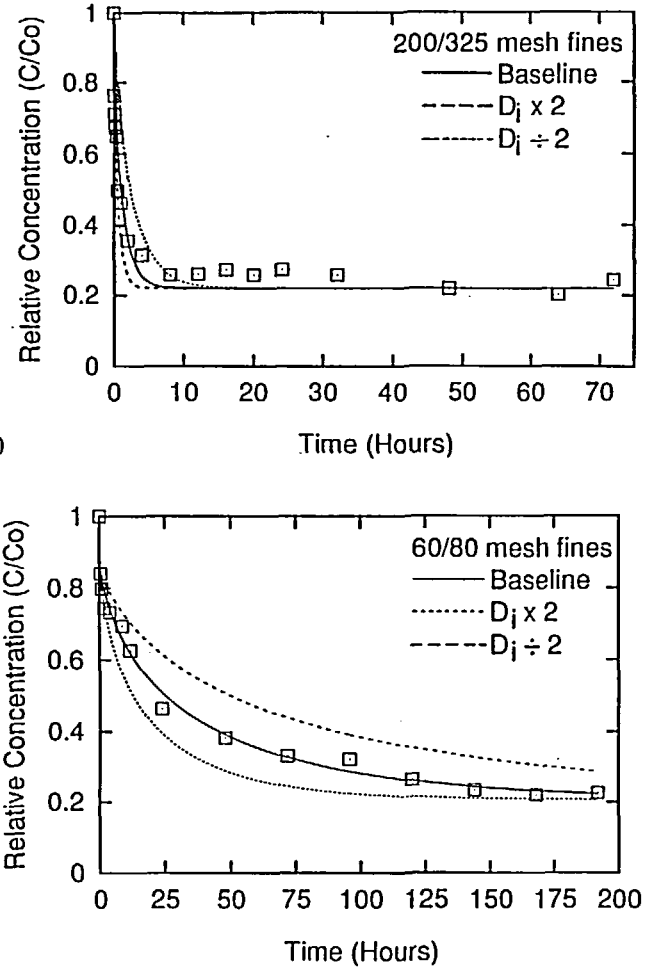

FIG. 8 Sensitivity of dual rate model simulations to D_i for (a) 200/325 mesh fines (baseline value of $D_i = 1.5 \times 10^{-10}$ cm²/s); and (b) 60/80 mesh fines (baseline value of $D_i = 3.5 \times 10^{-11}$ cm²/s).

CONCLUSIONS

The kinetics of cadmium adsorption by recycled shot blast fines has been investigated. Adsorption rates are fairly rapid for powdered (i.e.,

200/325 mesh) fines, with 90% or more of the removal occurring within 5–10 hours. In tests with larger (granular) particle sizes, there was rapid initial removal followed by a slow and lengthy approach toward the equilibrium position. Batch rate data were analyzed by both a surface reaction model and a dual rate mass transfer model. Dual rate model simulations provided a better description of the data for small particle sizes, but simulations using the two models converged for 60/80 mesh (~0.21 mm diam.) and larger sorbent particles. Both the intraparticle diffusion coefficient of the dual-rate formulation and the surface reaction rate constant varied with the inverse of the particle radius, confirming a diffusion- versus surface reaction-limited adsorption rate.

The results taken together suggest the use of the powdered-sized fines in batch mode for cadmium removal. The density of the fines, on the order of sand or gravel, should promote effective solids separation at the termination of the reaction. The presence of colloidal iron, however, may necessitate coagulation to remove it entirely from solution. This issue warrants further study since some cadmium may be associated with the colloidal iron, thereby underestimating the sorption capacity, assuming that it passes through the 0.45-μm filter and is subsequently analyzed. If colloidal iron generation is considerably less for the 30/40 mesh fraction versus the smaller sizes, this would help explain the variations in apparent adsorption capacity between these fractions. While this will likely not alter the kinetic patterns or even the rate constants associated with the respective size fractions, it affords a more complete and accurate picture of mass transport relative to the recycled fines and their application.

The larger sorbent particles are likely best utilized in flow through (e.g., fixed bed) applications given the slower, diffusion-limited approach to equilibrium. The relatively low values of the intraparticle diffusion coefficient, however (on the order of 10^{-11} cm^2/s), may mean that the mass transfer zone will be large, requiring a substantial bed depth to contain the zone for high quality effluent requirements. This may be offset somewhat given the rather flat slope of the adsorption isotherm as reflected in the Freundlich exponent, n. Column studies are needed to determine the extent to which batch kinetic information characterizes the performance of fixed beds for removal of cadmium by the recycled iron material.

NOMENCLATURE

C	liquid-phase concentration (M-pollutant/L^3)
C_e	equilibrium liquid-phase concentration (M-pollutant/L^3)
C_0	initial liquid-phase concentration (M-pollutant/L^3)

C_s liquid-phase concentration at particle surface (M-pollutant/L^3)
D_i intraparticle diffusion coefficient (L^2/t)
K_{ads} equilibrium constant for surface complexation reaction
K_F Freundlich isotherm constant [$(L^3)^n$(M-pollutant)$^{1-n}$/M-solid]
k_f external film diffustion coefficient (L/t)
K_{si} surface protolysis constant
k_s surface reaction rate coefficient (L/t)
n Freundlich isotherm exponent
Q solid-phase concentration (M-pollutant/M-solid)
Q_{avg} average concentration of sorbate in sorbent (M-pollutant/M-solid)
Q_e equilibrium solid-phase concentration (M-pollutant/M-solid)
r radial distance in sorbent particle (L)
V reactor volume (L^3)
W_c mass of sorbent (M-solid)
ρ density of sorbent particle (M-solid/L^3)

ACKNOWLEDGMENTS

The laboratory assistance of Dameon Booker and Preston Poulter is gratefully acknowledged. This material is based in part upon work supported by Tyler Pipe Co., Tyler, Texas; the Texas Advanced Technology Program under Grant 3613009; and the US EPA Risk Reduction Engineering Laboratory under Cooperative Agreement CR 821824-01-0. The views presented do not necessarily represent those of the supporting agencies, and the mention of trade names does not constitute endorsement. Patents on processes and materials described herein have been issued or are pending.

REFERENCES

1. C. P. Schulthess and C. P. Huang, "Adsorption of Heavy Metals by Silicon and Aluminum Oxide Surfaces on Clay Minerals," *Soil Sci. Soc. Am.*, *54*, 679–687 (1990).
2. C. Blanchard, M. Manuanyl, and G. Martin, "Removal of Heavy Metals from Waters by Means of Natural Zeolites," *Water Res.*, *18*, 1501–1507 (1984).
3. D. G. Kinniburgh and M. L. Jackson, "Cation Adsorption by Hydrous Metal Oxides and Clays," in *Adsorption of Organics at Solid–Liquid Interfaces* (M. A. Anderson and A. J. Rubin, Eds.), Ann Arbor Science, Ann Arbor, MI, 1981, pp. 91–160.
4. Y. Gao, A. K. Sengupta, and D. Simpson, "A New Hybrid Inorganic Sorbent for Heavy Metals Removal," *Water Res.*, *29*, 2195–2205 (1995).
5. H. Fan and P. R. Anderson, "Development and Evaluation of Mn Oxide-Coated Composite Adsorbent for the Removal and Recovery of Heavy Metals from Metal Contami-

nated Wastewater," in *Proceedings 50th Industrial Waste Conference, Purdue University*, Ann Arbor Press, Ann Arbor, MI, 1995, pp. 217–226.
6. N. C. Das and M. Bandyopadhyay, "Removal of Copper(II) Using Vermiculite," *Water Environ. Res.*, *64*, 852–857 (1992).
7. O. J. Hao, C. M. Tsai, and C. P. Huang, "The Removal of Metals and Ammonium by Natural Glauconite," *Environ. Int.*, *13*, 203–212 (1987).
8. E. L. Bagby, "Treatment of an Anionic Metal by Adsorption on Iron Oxides," in *Emerging Technologies in Hazardous Waste Management V*, ACS, Washington D.C., 1993, p. 318.
9. M. F. Schultz, M. M. Benjamin, and J. F. Ferguson, "Adsorption and Desorption of Metals on Ferrihydrite," *Environ. Sci. Technol.*, *21*, 863–869 (1987).
10. J. M. Zachara, D. C. Girvin, R. L. Schmidt, and C. T. Resch, "Chromate Adsorption on Amorphous Iron Oxyhydroxide in the Presence of Major Groundwater Ions," *Ibid.*, *21*, 589–594 (1987).
11. M. M. Benjamin, "Adsorption and Surface Precipitation of Metals on Amorphous Iron Oxyhydroxide," *Ibid.*, *17*, 686–692 (1983).
12. T. L. Theis, R. Iyer, and S. K. Ellis, "Evaluating a New Granular Iron Oxide for Removing Lead from Drinking Water," *J. Am. Water Works Assoc.*, *84*(7), 101–105 (1992).
13. W. R. Knocke, S. C. Occiano, and R. Hungate, "Removal of Soluble Manganese by Oxide-Coated Filter Media," *Ibid.*, *83*(8), 64–69 (1991).
14. M. Edwards and M. M. Benjamin, "Adsorptive Filtration Using Coated Sand: A New Approach for Treatment of Metal-Bearing Wastes," *J. Water Pollut. Control Fed.*, *61*, 1524–1533 (1989).
15. E. H. Smith, "Uptake of Heavy Metals in Batch Systems by a Recycled Iron-Bearing Material," *Water Res.*, *30*, 2424–2434 (1996).
16. S. Kesraoui-Ouki, C. Cheeseman, and R. Perry, "Effects of Conditioning and Treatment of Chabazite and Clinoptilolite Prior to Lead and Cadmium Removal," *Environ. Sci. Technol.*, *27*, 1108–1116 (1993).
17. S. Sengupta and A. K. Sengupta, "Characterizing a New Class of Sorptive/Desorptive Ion Exchange Membranes for Decontamination of Heavy-Metal-Laden Sludges," *Ibid.*, *27*, 2133–2140 (1993).
18. M. O. Corapcioglu and C. P. Huang, "The Adsorption of Heavy Metals onto Hydrous Activated Carbon," *Water Res.*, *21*, 1030–1044 (1987).
19. T. D. Mayer and W. M. Jarrell, "Formation and Stability of Iron(II) Oxidation Products under Natural Concentrations of Dissolved Silica," *Ibid.*, *30*, 1208–1214 (1996).
20. X. Meng and R. D. Letterman, "Effect of Component Oxide Interaction on the Adsorption Properties of Mixed Oxides," *Environ. Sci. Technol.*, *27*, 970–975 (1993).
21. E. H. Smith, *Research with Waste Shot Blast Fines from Cast-Iron Manufacturing Processes—Progress Report*, Mechanical Engineering Department, Southern Methodist University, 1994.
22. J. M. Smith, *Chemical Engineering Kinetics*, 3rd ed., McGraw-Hill, London, 1981.
23. E. L. Cussler, *Diffusion: Mass Transfer in Fluid Systems*. Cambridge University Press, London, 1984.
24. P. W. Schindler and W. Stumm, "The Surface Chemistry of Oxides, Hydroxides, and Oxide Minerals," in *Aquatic Surface Chemistry* (W. Stumm, Ed.), Wiley, New York, NY, 1987.

Received by editor July 25, 1996
Revision received June 1997